

Wireless induction charging station for industrial applications

1st Pēteris Aizpurietis
Institute of Electronics and Computer Science
Riga, Latvia
peteris.aizpurietis@gmail.com

2nd Didzis Lapsa
Institute of Electronics and Computer Science
Riga, Latvia
didzis.lapsa@edi.lv

3rd Niklāvs Barkovskis
Institute of Electronics and Computer Science
Riga, Latvia
niks.barkovskis@gmail.com

4th Arnis Salmiņš
Institute of Electronics and Computer Science
Riga, Latvia
arnis.salms@gmail.com

5th Rims Janeliukštis
Institute of Electronics and Computer Science
Riga, Latvia
<https://orcid.org/0000-0002-0374-5441>

6th Kaspars Ozols
Institute of Electronics and Computer Science
Riga, Latvia
kaspars.ozols@edi.lv

Abstract— Wiring for charging LiPo batteries poses problems due to electromagnetic interference and limitations of wire length. In this work, a method for charging wireless sensor network wirelessly using NRF52840 is developed for both transmitting and receiving side of equipment. A Qi-compliant WE760308103202 wireless charging coil receiver is used and its performance evaluated to estimate optimal parameters of wireless charging, such as load and resonance frequency detuning for receiver. By tuning the frequency of operation, it is possible to utilize generic electronic components with reduced costs.

Keywords— wireless charging, sensor network, parameter optimization

I. INTRODUCTION

Main quality of a wireless sensor network (WSN) node is the ability to perform wirelessly. Device for both energy and information transfer has been outlined as early as in works of Nikola Tesla [1]. However recently, in last couple of decades, near field non-radiant energy transfer has greatly gained in popularity where energy transfer is conducted by utilizing low frequency (tens of kHz) evanescent magnetic field tails for loosely coupling inductors of LC resonator tanks [2].

Non-radiant near-field energy transfer differs from already established methods of contactless power transfer such as magnetic coupling (e.g. magnetic core transformer) which demands transfer distance to be nil in contrast of transfer distances of allowed few lengths of greatest dimension of transducer (inductor's diameter) or from radiant far-field energy transfer (e.g. microwave beam, with strict constraints of human exposure, requiring line of sight for operation [3]) in contrast to low frequency magnetic fields that interact weakly with non-magnetic materials (human flesh) as can be seen in IEEE standard for safety levels for human exposure aka Std C95.1 [4] where far greater magnetic field strength and power density contained in low frequency fields (frequencies utilized in near-field non-radiant energy transfer) are allowed.

Implementing this wireless charging feature in already existing WSN that of an IMECH project [5], readily available hardware (nRF52840 Cortex-M4) and communication channels (Bluetooth radiolink) were both deployed together with cheap and nonspecific power electronics. Considering the fact that the sensor node is located on a rotating attachment, it is not possible to connect charging wires, so one of the most convenient charging solutions is wireless

charging, without taking into account the transmission power losses. However, received power must sustain this relatively low power application. As of portability, certain arbitrariness of position is defined by specifying maximum clearance between node and power pad to be 10 cm with defined charging power as that of a low-power Li-Po charger MCP73831T, 15-500mA, or say as that of a low power USB2.0 device, 5V 100mA.

There is no plethora of readily available solutions that would allow for simplicity and clearance (10 cm), however wide variety of commodities – controllers, switching circuitry, wireless power transfer (WPT) inductors are at disposal. Readily available solutions such as Qi protocol could not be applied because of insufficient data channel which in Qi is based on inductive [6] coupling (same as NFC which supports communication only up to 4 cm [7]). Feedback data are transferred by changing receiver's impedance (usually adding to LC tank's capacity) thus affecting transmitter's LC tank's amplitude from which data can be recovered by signal processing. Thus data link is disrupted as received power becomes unusable. This is unsatisfying situation for WSN node attached to a mobile system that could change its position for better charging.

II. MATERIALS AND METHODS

Electrical circuitry of the proposed charging system is presented in Figure 1. The charging system is constituted of a WSN node as a power recipient and charging station (a power transmitter). The node utilizes WE760308163202 coil (mass-produced for exactly this purpose) as inductance of receiving resonance tank. The node's main power consumer (current required for operation of nRF52840 can be of 5 V few mA and for wireless transmission with max power rarely exceeds 10 mA) is LiPo charging controller operating mostly in constant current mode, which can be deliberately enabled and is set to 100 mA. In Figure 1, k is the coupling factor and M is mutual coupling between coils.

Charging station utilizes coaxial coplanar (pancake) coil with a diameter of approximately 0.15 m. Low-loss capacitors had to be acquisitioned to dampen the heat generation that emerged at even as little as 10 Watts of reactive load at transmitter's resonance tank.

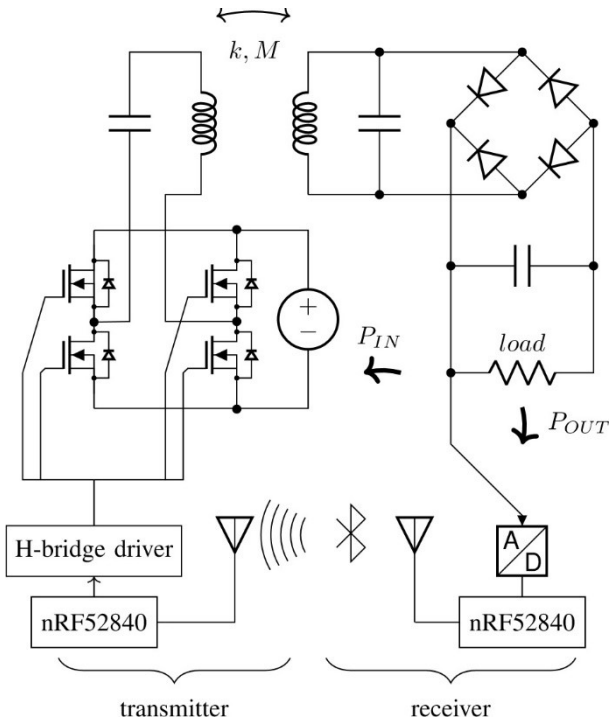


Fig. 1. The proposed wireless charging system.

A. Hardware

Transmitter side consists of LC tank with inductor whose magnetic field lines are exempted in receiver's direction. Electromotive force (EMF) induced in receiver's LC tank depends on both, mutual position between charger and receiver and on reactive load under which transmitter's LC tank is running. Because of necessity of controlling the EMF a feedback over Bluetooth was utilized to keep constant voltage past receiver's rectifier. This was done partly for overvoltage protection of receiving circuitry [6] because voltage after rectifier can easily exceed several tens of volts even for small changes in charging distance.

Reactive load of transmitter's tank is proportional-integral-derivative (PID) controlled by altering amount of current pumped into LC contour via phase-shifted full bridge (PSFB) circuitry [8] setting the phase shift [9]. As will be seen in receiver inductor's performance evaluation, 5 V after rectifier is a reasonable target value for control process of the discussed coil.

B. State machine

Flowchart of the proposed charging algorithm is shown in Figure 2. State machine of a charging system was realized in transmitter's NRF52840 controller with a control loop - linear function of high priority in main loop - callback after timer event (each 50 ms). This control loop consists of assessing and updating a system state (waiting, operation, fault), of evaluating PID equation and accordingly setting reactive load of LC tank by setting phase shift in PSFB driver which was implemented using 2 timer peripherals and a software interrupt. PID was fed ADC data that was received over Bluetooth with a refresh rate of 10 Hz.

Wireless power transfer process was initiated with charging system starting in waiting mode while sending analog ping. This is done by setting PSFB controller to deliver certain power for 50 ms once in a second. If power receiver is in reception range, voltage pulses past rectifier

exceed certain threshold. Following that, PID process is launched and voltage after rectifier stabilizes to target value (5 volts). Then WSN node would enable its main consumer LiPo charger which was set to 100 mA constant current mode. Voltage after rectifier is usually sustained as it is expected.

If PID control reaches maximum phase shift value of PSFB which basically means that PID is able no longer to control, fault condition is raised and charging station falls back to waiting state altogether with setting timeout for new charging event.

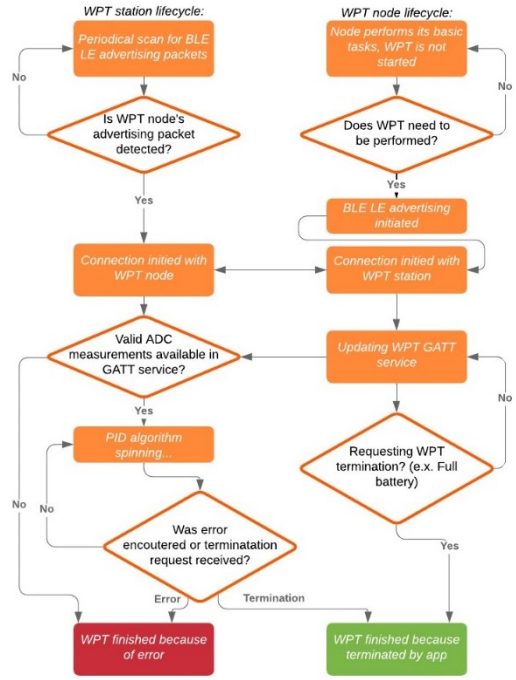


Fig. 2. The proposed wireless charging algorithm.

III. RESULTS AND DISCUSSION

Problems of maximizing received power and maintaining power transfer efficiency while varying charging distance are addressed by application of simple and crude models such as impedance matching model of ac power source [10]. This model balances expectations of received power and the available voltage in combination with the coupled resonators model [11-13], which describes how changes of coupling of resonators (for example, changes in transfer distance) affect frequency at which maximum forward gain (transfer efficiency) is achieved. Applying those models to data is used to get an estimate of overall performance of the system and its applicability in certain scenarios. i.e. show feasible range of operation for charging distance or amount of frequency detuning due to, again, distance variance.

A. Optimum load – internal resistance model

Jackobi's law states that the maximum external power from source can be obtained when resistance of load matches that of the source [14]. Optimal working point for various clearances h for commercially available coil - WE760308103202 - can be estimated by testing it against charger's LC tank's inductor under constant reactive load. Operating frequency being 63 kHz, whilst testing the receiver coil against stationary alternating magnetic field created by a flat inductor, varying load was applied after rectifier and sufficient bypass capacitor and data was fitted to internal resistance model.

Impedance matching method based on maximum power transfer principle can be applied to many WPT configurations regardless of number of members [15]. WPT can be represented as an equivalent circuit of an AC power source shown in Figure 3.

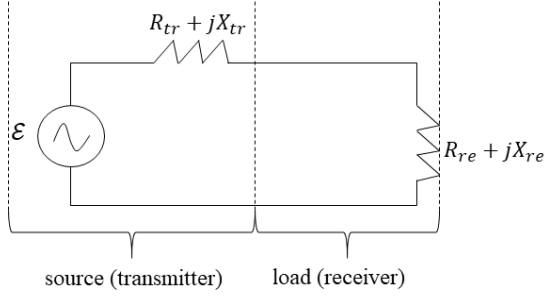


Fig. 3. Electrical circuit of a charging system.

The EMF can be expressed as

$$\mathcal{E} = I(R_{tr} + jX_{tr}) - I(R_{re} + jX_{re}), IR_L = \mathcal{E} \quad (1)$$

In most favorable (reactance-wise) conditions, a relation

$$\mathcal{E} = I(R_{tr} + R_{re}) \quad (2)$$

holds true and an output power

$$P = R_{re} \left(\frac{\mathcal{E}}{R_{re} + R_{tr}} \right)^2 \quad (3)$$

tops when $R_{tr} = R_{re}$ condition is met.

In each situation it is beneficiary to know the optimum load for the maximum power reception and output voltage at which this condition is met. Data obtained from testing receiver's coil for various transmission distances was fitted to the internal resistance model. As can be seen in Figure 4 and Figure 5, data complies with the model.

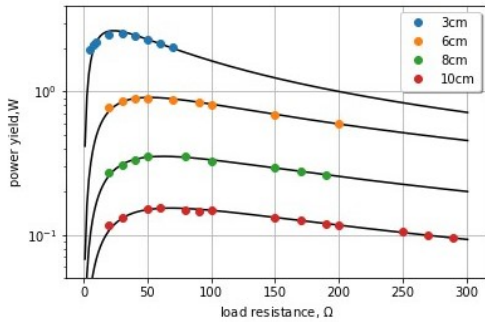


Fig. 4. Received power versus the applied load for different charging distances. The black lines represent the trendlines obtained from an internal resistance model.

EMF induced in receiver's coil is expressed as

$$\mathcal{E} = -M \frac{dI_{tr}}{dt} = k \sqrt{L_{re} L_{tr}} \frac{dI_{tr}}{dt} \quad (4)$$

where M is mutual inductance, I_{tr} is current induced in the transmitter coil, L_{re} is an inductance of a receiving coil, L_{tr} is an inductance of a transmitting coil and k is a coupling factor for coaxial coplanar coils. According to [16], the coupling factor is equal to

$$k = \left(1 + 2^{2/3} \frac{h^2}{r_1 r_2} \right)^{-3/2} \quad (5)$$

where r_1 and r_2 are the radii of receiving and transmitting coils, respectively and h is the transfer distance. Symbolically k as a factor of mutual impact between the coils is depicted in Figure 1.

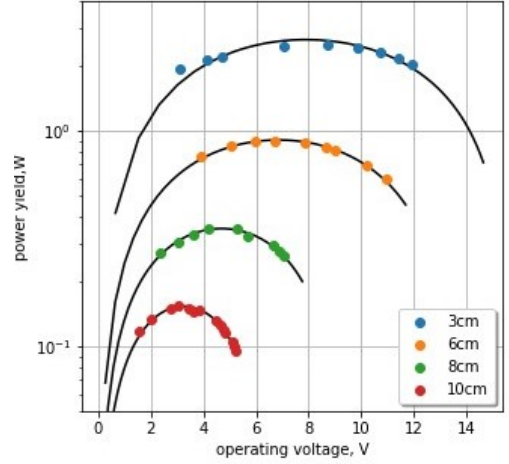


Fig. 5. Received power versus available voltage (RMS) for different charging distances. The black lines represent the trendlines obtained from an internal resistance model.

By substituting Equation (5) into Equation (4), the EMF can be rewritten as

$$\mathcal{E} = \sqrt{L_{re} L_{tr}} \frac{dI_{tr}}{dt} \left(1 + 2^{2/3} \frac{h^2}{r_1 r_2} \right)^{-3/2} \quad (6)$$

This model where induced EMF is dependent exclusively on k (so-called k -model), fits better for describing inductive coupling rather than resonant inductive coupling because in latter case influence of mutual coupling M on resonance is to be taken into account. That would explain why that model follows data only approximately. The results of application of the k -model on the EMF and internal resistance data are shown in Figure 6.

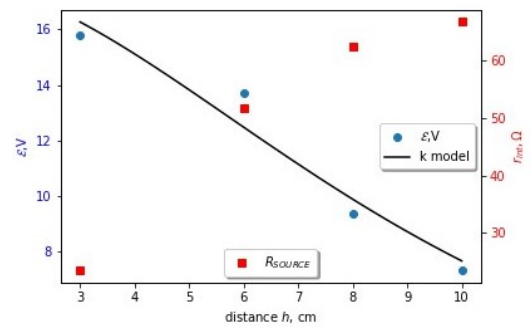


Fig. 6. Internal resistance and EMF of a source vs charging distance.

B. Optimum frequency – coupled resonators model

Frequency response of coupled resonators can be related in such an approximation of forward gain [11, 12]

$$\eta = \frac{k^2 Q_{tr} Q_{re} r_{re}}{(1+r_{re})(1+r_{re}+k^2 Q_{tr} Q_{re})+4 \left(\frac{\omega-\omega_0}{\omega} \right)^2 Q_{re}^2} \quad (7)$$

where ω is an angular frequency, $\omega_0 = \frac{1}{\sqrt{L_{tr}C_{tr}}} = \frac{1}{\sqrt{L_{re}C_{re}}}$ is the resonant frequency of the electrical resonator, $Q_{tr} = \omega_0 \frac{L_{tr}}{R_{tr}}$ and $Q_{re} = \omega_0 \frac{L_{re}}{R_{re}}$ are the quality factors of transmitting and receiving parts, respectively and $r_{re} = \frac{Z_{0,re}}{R_{re}}$ is an impedance ratio with $Z_{0,re}$ being a characteristic impedance of the transmission line in the cable between the load and receiving resonator.

It can be assumed that such systems independently of resonator count have almost identical relations of forward gain frequency. Experimental data was fitted to the coupled resonators model and the results are presented in Figure 7. As can be seen, frequency of system's top performance was observed to change, therefore it was concluded that frequency adaptation while in operation is crucial for performance [6] especially charging distance being subject to voluntary change.

WE760308103202 coil receiver was tested for optimum frequency with charger in feedback (i.e. normal operation, 5 V, 100 mA consumption on receiver's) mode for several charging distances. Experiment consisted of launching WPT system in normal operation mode i.e. PID process ensured 5 V behind receiver's rectifier where resistor of 50Ω was placed together with ceramic bypass capacitor of $10 \mu\text{F}$. On each of charging distances h a frequency sweep was launched. For each of the tested frequencies, a power transfer ratio $P_{\text{received}}/P_{\text{transmitted}}$ value was obtained (if working frequency diverges too much from system's resonance frequency, power transfer becomes impossible even with maximum phase shift of PSFB value). Values of charger's input voltage (which was constant 19.5 V) and current was logged with microcontroller together with voltage of the receiver (which was constant) so end to end efficiency could be estimated at once.

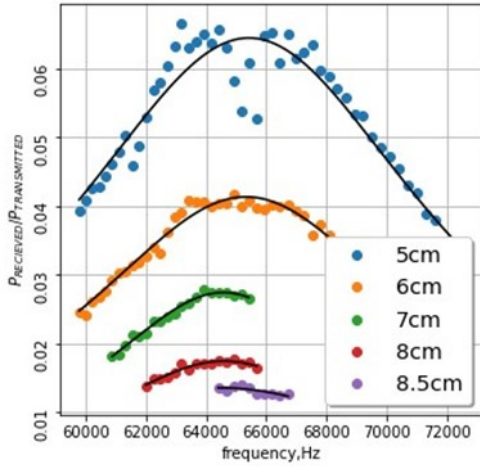


Fig. 7. Frequency of the best performance is detuned with change of charging distance. The black lines show trendlines obtained with the coupled resonators model.

An article of H. Sugiyama [13] describes a WPT system similar to ours. The resonant frequency of the system is

$$\omega_{res} = \sqrt{\frac{2CR^2 - L(1-k^2)}{2L(1-k^2)C^2R^2}} \cong \frac{1}{\sqrt{LC(1-k^2)}} \quad (8)$$

It describes frequency detuning dependent on the coupling parameter k . Here, L , C and R are inductance, capacitance and active resistance of either power reaches maximum. Experimentally obtained data was fitted to this model,

although resonant coils not being identical would render this approximation less precise. Equation (5) describing relation between the coupling parameter k and power transfer distance h was applied to our data. So that the Equation (8), in our case, can be rewritten as transmitting or receiving side, respectively. At this resonant frequency, the transmitted

$$\omega_{res} = \frac{(LC)^{-1/2}}{1 - \left(1 + 2^{2/3} \frac{h^2}{r_1 r_2}\right)^{-3/2}} \quad (9)$$

Equation (9) can be applied to assess the change of optimum frequency whilst changing the charging distance. The results are displayed in Figure 8. It can be seen that the optimum frequency is approximately inversely proportional to the charging distance.

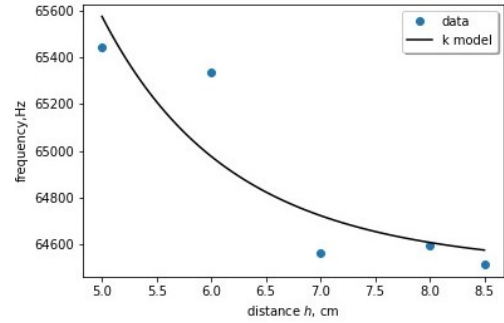


Fig. 8. Optimum frequency detuning versus charging distance. Approximately inverse proportionality can be seen.

Similarly, by combining Equation (5) with Equation (7), it is possible to express the transfer efficiency η as a function of the charging distance h :

$$\eta = \frac{\left(1 + 2^{2/3} \frac{h^2}{r_1 r_2}\right)^{-3} Q_{tr} Q_{re} r_{re}}{(1 + r_{re}) \left(1 + r_{re} + \left(1 + 2^{2/3} \frac{h^2}{r_1 r_2}\right)^{-3} Q_{tr} Q_{re}\right) + 4 \left(\frac{\omega - \omega_0}{\omega}\right)^2 Q_{re}^2} \quad (10)$$

Here, the transfer efficiency depends only on the charging distance and frequency, all other terms are constants. As can be seen in Figure 9, the result shows compatibility with the measured data.

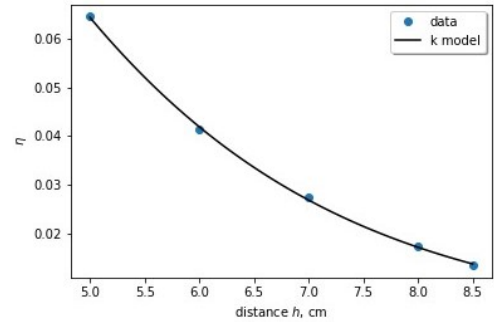


Fig. 9. End-to-end efficiency related to the charging distance.

CONCLUSIONS

1) The wireless induction charging system was developed using nRF52840 controllers in charging station and in receiver, h-bridge with drivers for transmitter's series resonance tank (with low loss capacitance for achieving higher Q-factor of contour) for charging station, and parallel resonance tank incorporating WE760308103202 wireless charging coil receiver for power recipient.

2) The purpose of this design was to allow arbitrariness of charging distance up to 10 cm, therefore non-radiant near-field energy transfer together with Bluetooth radiolink for feedback data was used as opposed to using only near-field for both energy and feedback data transfer. This approach enables a low latency control link.

3) Data, such as power levels measured at various frequencies and charging distances was fitted to the ac power source model in order to evaluate the performance of receiver (WE760308103202 coil). It was found that in the range of data considered device acts as ac power source yet with its electromotive force rapidly decreasing, while the source impedance rapidly increasing with charging distance.

4) The coupled resonators model was used for assessing deviation of the working frequency that would be optimum for energy transfer with changing charging distance. The model is partially applicable, however, perhaps another model is needed for frequency readjustment 'on the go' if charging distance was altered during the charging process.

5) A relatively simple wireless charging hardware can be used if the wireless sensor network nodes are positioned within 10 cm distance from the charger.

ACKNOWLEDGMENT

This work is the result of activities within the 'Intelligent Motion Control Platform for Smart Mechatronic Systems' (IMECH) project, which has received funding under the Horizon 2020 ECSEL Joint Undertaking (ECSEL-JU) grant agreement No. 737453. This Joint Undertaking received support from the European Union's Horizon 2020 research and innovation program and Czech Republic, Belgium, France, The Netherlands, Latvia, Spain, Italy, Greece, Portugal, Austria, and Ireland. The support is gratefully acknowledged.

REFERENCES

- [1] N. Tesla. Colorado Springs Notes 1899-1900, 1st ed.; Publisher: Nolit, Beograd, Yugoslavia, 1978.
- [2] A. Karalis, J.D. Joannopoulos and M. Soljačić, "Efficient wireless non-radiative mid-range energy transfer," *Ann. Phys.-New York* 2008, 323, pp. 34-48.
- [3] P. Kant, K. Dobrzyniewicz and J.J. Michalski, "Autonomous System of Wireless Power Distribution for Static and Moving Nodes of Wireless Sensor Networks," In *Wireless Power Transmission for Sustainable Electronics*, 1st ed; Editor 1, N. Borges Carvalho, Editor 2, A. Georgiadis; John Wiley & Sons, 2020; pp. 247-286.
- [4] IEEE Standard for Safety Levels with Respect to Human Exposure to Electric, Magnetic, and Electromagnetic Fields, 0 Hz to 300 GHz, IEEE Std C95.1-2019.
- [5] M. Čech, A.J. Beltman and K. Ozols, "IMECH-Smart System Integration for Mechatronic Applications," In *Proceedings of IEEE International Conference on Emerging Technologies and Factory Automation*, Zaragoza, Spain, September 10-13, 2019, pp. 843-850.
- [6] Qi Wireless Power Consortium The Qi Wireless Power Transfer System Power Class 0 Specification Parts 1 and 2: Interface Definitions. Version 1.2.3 February 2017.
- [7] Near-field communication. Available online: [en.wikipedia.org/wiki/Near-field communication](https://en.wikipedia.org/wiki/Near-field_communication) (accessed on March 18, 2022).
- [8] P. O'Neill, J. Zhang and W.G. Hurley, "A Phase-shifted Full-Bridge ZVS DC/DC Converter for Wireless Charging of Electric Vehicles," In *Proceedings of 50th International Universities Power Engineering Conference (UPEC)*, Stoke on Trent, UK, September 1-4, 2015, pp. 1-5.
- [9] A. Triviño-Cabrera, J.M. González-González and J.A. Aguado, *Design of the Power Converters. In Wireless Power Transfer for Electric Vehicles: Foundations and Design Approach*, 1st ed; Springer Nature Switzerland, 2020, pp. 129-152.
- [10] Y. Zhang, Z. Zhao and K. Chen, "Load matching analysis of magnetically-coupled resonant wireless power transfer," In *Proceedings of IEEE ECCE Asia Downunder*, Melbourne, Australia, June 3-6, 2013, pp. 788-792.
- [11] H. Hoang and F. Bien, "Maximizing Efficiency of Electromagnetic Resonance Wireless Power Transmission Systems with Adaptive Circuits," In *Wireless Power Transfer - Principles and Engineering Explorations*, 1st ed; Editor Ki Young Kim; IntechOpen, 2012; pp. 207-226.
- [12] T. Komaru, M. Koizumi, K. Komurasaki, T. Shibata, and K. Kano, "Compact and Tunable Transmitter and Receiver for Magnetic Resonance Power Transmission to Mobile Objects," In *Wireless Power Transfer - Principles and Engineering Explorations*, 1st ed; Editor Ki Young Kim; IntechOpen, 2012; pp. 133-150.
- [13] H. Sugiyama, *Performance Analysis of Magnetic Resonant System Based on Electrical Circuit Theory. In Wireless Power Transfer - Principles and Engineering Explorations*, 1st ed; Editor Ki Young Kim; IntechOpen, 2012; pp. 95-116.
- [14] Maximum power transfer theorem. Available online: [en.wikipedia.org/wiki/Maximum power transfer theorem](https://en.wikipedia.org/wiki/Maximum_power_transfer_theorem) (accessed on March 22, 2022).
- [15] S.Y.R. Hui, W.X. Zhong and C.K. Lee, "A Critical Review of Recent Progress in Mid-Range Wireless Power Transfer," *IEEE T. Power Electr.* 2014, 29, pp. 4500-4511.
- [16] J.T. Conway, "Inductance Calculations for Noncoaxial Coils Using Bessel Functions," *IEEE T. Magn.* 2007, 43, 3, pp. 1023-1034.